Bioorg. Med. Chem. 104 (2024) 117714

Contents lists available at ScienceDirect

Bioorganic & Medicinal Chemistry

journal homepage: www.elsevier.com/locate/bmc

Disclosure of cinnamic acid/4,9-diaminoacridine conjugates as multi-stage antiplasmodial hits

Mélanie Fonte [a], Catarina Rôla [b], Sofia Santana [b], Yunuen Avalos-Padilla [c,d], Xavier Fernàndez-Busquets [c,d,e], Miguel Prudêncio [b], Paula Gomes [a,*], Cátia Teixeira [a,1]

[a] LAQV-REQUIMTE, Departamento de Química e Bioquímica, Faculdade de Ciências, Universidade do Porto, Portugal
[b] Instituto de Medicina Molecular, Faculdade de Medicina, Universidade de Lisboa, Portugal
[c] Nanomalaria Group, Institute for Bioengineering of Catalonia (IBEC), The Barcelona Institute of Science and Technology, Spain
[d] Barcelona Institute for Global Health (ISGlobal, Hospital Clínic-Universitat de Barcelona), Spain
[e] Nanoscience and Nanotechnology Institute (IN2UB), University of Barcelona, Spain

ARTICLE INFO

Keywords:
Antimalarial
Cinnamic acid
Covalent bitherapy
Diaminoacridine
Multi-target

ABSTRACT

4,9-diaminoacridines with reported antiplasmodial activity were coupled to different *trans*-cinnamic acids, delivering a new series of conjugates inspired by the covalent bitherapy concept. The new compounds were more potent than primaquine against hepatic stages of *Plasmodium berghei*, although this was accompanied by cytotoxic effects on Huh-7 hepatocytes. Relevantly, the conjugates displayed nanomolar activities against blood stage *P. falciparum* parasites, with no evidence of hemolytic effects below 100 μM. Moreover, the new compounds were at least 25-fold more potent than primaquine against *P. falciparum* gametocytes. Thus, the new antiplasmodial hits disclosed herein emerge as valuable templates for the development of multi-stage antiplasmodial drug candidates.

1. Introduction

Malaria is a life-threatening infectious disease caused by protozoan parasites of the genus *Plasmodium*. Six species of *Plasmodium* can infect humans, *Plasmodium falciparum* and *P. vivax* being the most prevalent in tropical and sub-tropical countries, where malaria represents a major health concern. While progress has been made in reducing malaria cases and deaths globally, complete eradication remains a complex and challenging goal.[1] The continued malaria burden is mainly due to (i) the complex parasite's life cycle, which undermines the prompt and successful development of effective drugs and vaccines, and (ii) the quick emergence and spread of drug-resistant strains of the parasite, compromising the efficacy of all the drugs developed so far.[1–3] Indeed, effective therapeutic options are becoming scarce since the current frontline artemisinin-based combination therapies (ACT) are facing a concerning decline in their effectiveness.[4–8] This highlights the urgent need to produce new potent antiplasmodial drugs that, ideally, overcome emerging drug resistance, whilst considering safety, especially in children and pregnant women, and improved dosing convenience.[9–11] Over the past decade, there has been significant attention directed towards multi-stage drugs, driven by their advantages in addressing complex diseases like malaria and issues related to drug resistance.[12–14] Since malaria mostly affects low-income populations, the challenge lies precisely in finding an affordable medicine that addresses all the desired characteristics. Most antimalarial drugs lack a clear and undisputed mechanism of action (MOA), which hampers the rational design of new drugs. Therefore, the development of antimalarials has been targeting the functionalization of existing pharmacophores, aiming at their re-

Abbreviations: ACT, Artemisinin-based combination therapies; ATP, adenosine triphosphate; CA, cinnamic acid; CQ, Chloroquine; DCM, dichloromethane; DIEA, *N,N*-diisopropylethylamine; DMSO, dimethyl sulfoxide; DNA, deoxyribonucleic acid; ESI-IT MS, electrospray ionization-ion trap mass spectrometry; HEPES, 4-(2-hydroxyethyl)-1-piperazine ethanesulfonic acid; HPLC-DAD, high-performance liquid chromatography with diode-array detection; IC_{50}, half-maximal inhibitory concentration; MOA, mechanism of action; n.d., not determined; NMR, nuclear magnetic resonance; *P.*, *Plasmodium*; PQ, Primaquine; QN, Quinacrine; RPMI, roswell Park Memorial Institute 1640 medium; RT, retention time; SAR, structure and activity relationship; SD, standard deviation; TBTU, O-(Benzotriazol-1-yl)-*N,N,N′,N′*-tetramethyluronium tetrafluoroborate; TLC, thin layer chromatography.

* Corresponding author.
E-mail address: pgomes@fc.up.pt (P. Gomes).
[1] Current affiliation: Gyros Protein Technologies Inc., Tucson, Arizona, USA.

https://doi.org/10.1016/j.bmc.2024.117714
Received 26 February 2024; Received in revised form 21 March 2024; Accepted 2 April 2024
Available online 3 April 2024

introduction in the chemotherapy repository.[15–18] Thus, several research groups, including ours,[19–30] have been dedicated to the rescuing of traditional antimalarial drugs such as quinacrine (QN), primaquine (PQ), and chloroquine (CQ), whose use has been limited due to resistance and/or toxicity issues.[17,31,32] QN was the first effective synthetic antimalarial drug with blood-schizonticidal activity. However, due to its severe side effects, QN was soon overtaken by CQ, a low-cost medicine with higher efficiency, oral bioavailability, and safety. Yet, due to the rise and spread of CQ-resistant strains of *P. falciparum*, its use has been progressively abandoned.[33,34] While QN and CQ target blood-stage parasites, as do most of the available antimalarials, PQ is, alongside tafenoquine (TQ),[35] the only drug capable of eliminating (i) liver forms of *Plasmodium* species, including the dormant hypnozoites of *P. vivax* and *P. ovale* that may induce malaria relapses, and (ii) gametocytes, preventing transmission to the mosquito vector. Nevertheless, PQ exhibits high hemotoxicity and limited oral bioavailability, which restricts its clinical use.[36,37].

We recently developed a family of compounds where the pharmacophores of QN, CQ and PQ are merged into a single 4,9-diaminoacridine core (**1a-b**, Figure 1), as potential multi-stage antiplasmodials.[23,38] The best compounds of this family, **1a** and **1b**, retained the activities of the parent drugs, PQ and CQ, displaying substantial *in vitro* activity against both the blood and liver stages of malaria parasites.[23] Inspired by these encouraging results and by former findings in our group,[24–30,39,40] we have now conjugated **1a** and **1b** to *trans*-cinnamic acids (CAs), targeting new conjugates with improved multi-stage efficacy and safety, and less propensity to develop resistance. This conjugation strategy was inspired in the covalent bitherapy concept pioneered by Meunier, whose combination of two pharmacophores in one single chemical entity has been widely and successfully employed, including in the context of antimalarial drug development.[41,42] The choice of CAs as the ancillary bioactive moiety was based on their ability to cause, in *Plasmodium* parasites, (i) a decline in energy production (ATP) due to the inhibition of lactate transporters, and (ii) a change in mitochondrial respiration; in addition, CAs have been reported to reduce the translocation of amino acids and carbohydrates in *Plasmodium*-infected erythrocytes.[40,43–45] Moreover, due to their α,β-unsaturated carbonyl moiety, CAs may act as Michael acceptors inhibiting cysteine proteases, especially falcipain-2 and falcipain-3, which also have a crucial role in hemoglobin degradation, the blood stage parasite's primary food source.[44,46–48] Therefore, we have coupled **1a** and **1b** to four different CAs, selected on the basis of the electronic properties and positions of substituents in the CA's aromatic ring, and assessed the efficacy of the resulting conjugates (**2**, Figure 1) against the liver, blood, and gametocyte stages of *Plasmodium* parasites *in vitro*. Data obtained shows that the new conjugates have enhanced multi-stage activity, especially against blood stage parasite forms, compared to the parent 4,9-diaminoacridines.

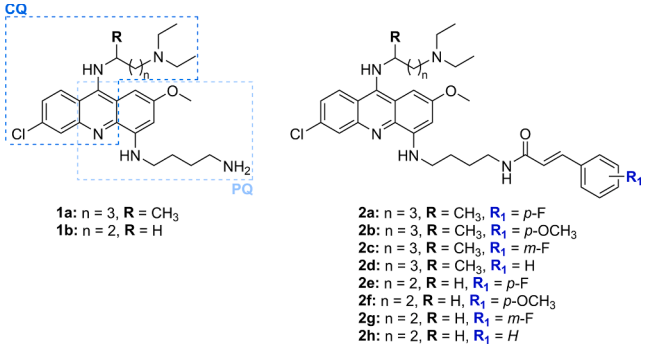

Figure 1. Dual-stage antiplasmodial 4,9-diaminoacridines (**1a,b**) previously developed by us,[23,38] and their cinnamic acid conjugates herein reported.

2. Results and discussion

2.1. Chemistry

The synthesis of target compounds **2a-h** was accomplished using the route outlined in Scheme 1**.** Detailed procedures and relevant spectroscopic data of the final compounds are provided in the Experimental Section, and the corresponding chromatographic and spectral traces are given in the Supporting Information (SI).

4,9-diaminoacridine derivatives **1a** and **1b** were first obtained by a seven-step synthetic route developed and optimized by us,[38,49] starting from methyl 2-amino-4-chlorobenzoate and 4-bromo-3-nitroanisole, as formerly described. Then, a classical *in situ* amide coupling method was used to couple **1a** and **1b** to a range of CAs, resulting in the synthesis of the target compounds **2a-h** (Scheme 1). For this purpose, the carboxylic acid group of each CA was initially activated in dichloromethane (DCM) for 1 h using *O*-(Benzotriazol-1-yl)-*N,N,N′,N′*-tetramethyluronium tetrafluoroborate (TBTU) and *N*-ethyl-*N,N*-diisopropylamine (DIEA) as a coupling agent and base, respectively. After the activation process, **1a** or **1b** was added to the mixture and the reaction proceeded at room temperature (r.t.) for approximately 4 h.

The target products were isolated by liquid chromatography on silica-gel columns in 94–98 % purity verified by high-performance liquid chromatography (HPLC). Structural analyses by electrospray ionization-ion trap mass spectrometry (ESI-IT MS), and by proton (^{1}H) and carbon-13 (^{13}C) nuclear magnetic resonance (NMR) validated the anticipated structures for all target compounds **2a-h**, which were achieved with moderate to good (24–82 %) overall yields.

2.2. Biological assays

2.2.1. Blood stage activity

The efficacy of the compounds against blood-stage parasites of the *P. falciparum* 3D7 strain was assessed *in vitro* using flow cytometry, as described in the Experimental Section. The results obtained are summarized in Table 1 and show that all conjugates **2a-h** were active against the blood forms of *P. falciparum* (3D7 strain). Although none of the compounds presented a similar or better activity than that of CQ, all of them were much better than the parent drugs **1a** and **1b**, showing IC_{50} values in the nanomolar range. This result was not unexpected, as conjugates **2a-h** are analogues of QN, conserving a basic aminoalkyl chain linked to the C-9 of the acridine ring that is relevant to the accumulation of QN in the parasite's acidic digestive vacuole where it inhibits hemozoin formation. This process is vital for the parasite as a mechanism for the detoxification of the free heme group released upon hemoglobin digestion.[50–54] Additionally, these conjugates possess a CA moiety known to affect other vital processes in the asexual intra-erythrocytic stages of *Plasmodium*, as already highlighted in the Introduction. The relevance of the basic aminoalkyl substituent in the acridine's C-9 position on the blood stage activity is further supported by the fact that conjugates **2a-h** were also considerably more potent than similar CA conjugates of 4-aminoacridines previously reported by us (**3a–d**, Figure 2 and Table 1),[39] in which lack such substituent.

The IC_{50} values obtained for the new conjugates **2a–h** were dependent on (i) the substituent of the aryl ring in the cinnamoyl building block (R_1) and (ii) the length of the amino side chain on the C-9 of the acridine ring (R and n). In this regard, the following observations can be noted:

(a) a shorter side chain in the acridine's C-9 (n = 2, **2e–h**) improved activity independently of the substituent (R_1) in the aryl ring of the cinnamoyl moiety; this trend had already been observed for the parent 4,9-diaminoacridines, where **1b**, with the shorter side chain, displayed a lower IC_{50} value ($IC_{50} = 0.44 \pm 0.21$ μM) than **1a** ($IC_{50} = 0.68 \pm 0.24$ μM);

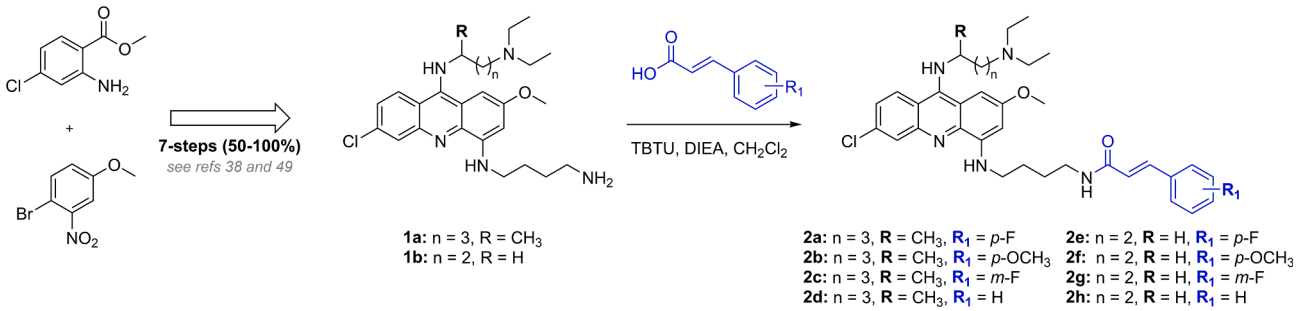

Scheme 1. Synthetic route to target compounds **2a-h**. 4,9-diaminoacridines **1a** and **1b** were first obtained in seven reaction steps starting from methyl 2-amino-4-chlorobenzoate and 4-bromo-3-nitroanisole, as previously described,[38,49] and next coupled to different CAs (highlighted in blue) under the following conditions: relevant CA (1.1 equiv), TBTU (1.1 equiv), DIEA (2 equiv) and DCM at r.t.

Table 1
In vitro activity of the new conjugates **2a-h**, their parent compounds (**1a,b**)[23] and reference drugs CQ and PQ against liver forms of *P. berghei*, as well as early gametocytes and ring stages of *P. falciparum* 3D7 strain. Data previously reported for similar CA conjugates of 4-aminoacridines (**3a-d**)[39] is also included, for comparison.

Compound	R	n	R_1	IC_{50} ± SD, μM		
				Blood stage[a]	Liver stage[b]	Gametocyte stage[c]
1a	CH_3	3	–	0.68 ± 0.24[d]	11.02 ± 0.44[d]	–
1b	H	2	–	0.44 ± 0.21[d]	n.d.[e]	–
2a	CH_3	3	*p*-F	0.178 ± 0.005	n.d.[e]	0.645 ± 0.045
2b	CH_3	3	*p*-OCH_3	0.3478 ± 0.0006	n.d.[e]	–
2c	CH_3	3	*m*-F	0.1528 ± 0.0003	n.d.[e]	–
2d	CH_3	3	H	0.164 ± 0.003	n.d.[e]	0.474 ± 0.032
2e	H	2	*p*-F	0.1637 ± 0.0002	n.d.[e]	–
2f	H	2	*p*-OCH_3	0.1605 ± 0.0001	n.d.[e]	~0.43
2 g	H	2	*m*-F	0.143 ± 0.057	n.d.[e]	0.461 ± 0.031
2 h	H	2	H	0.0802 ± 0.0001	n.d.[e]	–
3a	–	–	*p*-F	5.83 ± 1.02[f]	0.884 ± 0.046[f]	–
3b	–	–	*p*-OCH_3	10.30 ± 1.40[f]	1.182 ± 0.115[f]	0.52 ± 0.38[f]
3c	–	–	*m*-F	4.34 ± 0.96[f]	0.561 ± 0.179[f]	0.14 ± 0.43[f]
3d	–	–	H	>70[f]	0.496 ± 0.230[f]	6.66 ± 1.54[f]
CQ	–	–	–	0.006 ± 0.004	–	–
PQ	–	–	–	–	8.428 ± 3.384	17.66 ± 2.31

[a] blood-stage antiplasmodial activity was determined against the CQ-sensitive *P. falciparum* 3D7 strain, using CQ as reference drug.
[b] liver-stage antiplasmodial activity was determined against liver forms of *P. berghei*, using PQ as reference drug.
[c] gametocytocidal activity was determined in *P. falciparum* NF54-gexp02-Tom strain, using PQ as reference drug.
[d] values taken from ref [23].
[e] n.d., not determined (toxic to Huh-7 cells at 10 μM).
[f] Values taken from ref [39].

(b) in the conjugates with the longer side chain (n = 3, **2a-d**), the results suggest that an electron-withdrawing group R_1, such as *p*-F (**2a**, IC_{50} = 0.178 ± 0.005 μM) and *m*-F (**2c**, IC_{50} = 0.1528 ± 0.0003 μM) is preferable to the electro-donating one (**2b**, IC_{50} = 0.3478 ± 0.0006 μM);
(c) changing the position of the aryl substituent from *para* to *meta*, as in **2a** (R_1 = *p*-F; IC_{50} = 0.178 ± 0.005 μM) *versus* **2c** (R_1 = *m*-F; IC_{50} = 0.1528 ± 0.0003 μM) or in **2e** (R_1 = *p*-F; IC_{50} = 0.1637 ± 0.0002 μM) *versus* **2 g** (R_1 = *p*-F; IC_{50} = 0.143 ± 0.057 μM), slightly improves activity;
(d) interestingly, the presence of a substituent in the aryl ring of the cinnamoyl moiety was not advantageous for blood stage activity of conjugates with the shorter side chain (**2e-h**), since the most potent compound of this sub-series was **2 h** (R_1 = H, IC_{50} = 0.0802 ± 0.0001 μM).

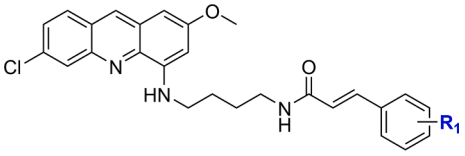

Figure 2. Cinnamic acid conjugates of 4-aminoacridines (**3a-d**) previously reported by us.[39]

Overall, conjugate **2 h** stood out for its higher activity against blood forms of *P. falciparum* (IC_{50} = 0.0802 ± 0.0001 μM), being approximately 5-fold more potent than its parent compound **1b** (IC_{50} = 0.44 ± 0.21 μM).

2.2.2. Hepatic stage activity

The effectiveness of conjugates **2a-h** against the hepatic stage of *P. berghei* parasites was assessed through a previously described bioluminescence-based method to quantify the *in vitro* parasite load of the human hepatoma (Huh-7) cell line.[55,56] Concomitantly, the cytotoxicity of the compounds towards this cell line was gauged by fluorescence-based assessment of cell confluency.

At the lowest concentration tested, 1 μM, the compounds did not effectively inhibit hepatic infection (Fig. 3). However, at 10 μM, all the compounds showed higher activity than PQ, the reference drug for this stage of infection. However, due to the high cytotoxicity displayed at this concentration, IC_{50} values were not determined and therefore no structure–activity relationships (SAR) could be inferred. Nevertheless, based on the impact that the introduction of the CA moiety had in conjugates **3a-d** and the lack of cytotoxicity of parent drugs **1a-b** at 10 μM (Fig. 3), we can hypothesize that the % of infection observed at this concentration for the new conjugates **2a-h** may be related to the incorporation of the CA moiety. However, further experiments are required to corroborate this hypothesis.

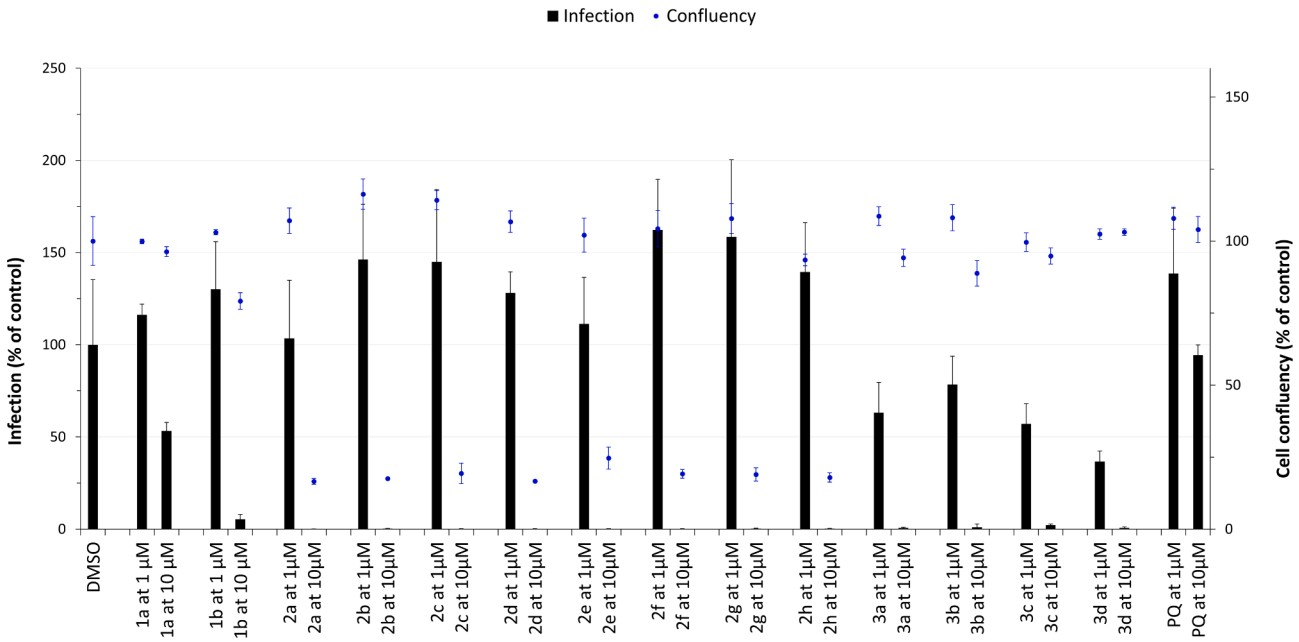

Figure 3. *In vitro* screening of the activity of conjugates **2a-h** and of their parent compounds **1a,b**[23] against liver forms of *P. berghei* (bars) and Huh-7 cells (dots) at 1 μM and 10 μM. Results previously obtained for CA conjugates of 4-aminoacridines **3a-d**[39] are included, for comparison. PQ was used as reference drug.

Relevantly, a comparison of the new CA conjugates of 4,9-diaminoacridines reported herein (**2a-h**) with their formerly disclosed analogues derived from 4-aminoacridines (**3a-d**),[39] shows that, while the presence of the aminoalkyl side chain in C-9 of the acridine ring has a clearly positive impact on blood stage activity (see previous section), the opposite happens in regard to toxicity to Huh-7 hepatocytes (Figure 3), as conjugates **3a-d** were not toxic to this cell line at 10 μM.[39].

Of note, owing to their ability to interact with DNA, among other MOA, many acridine-based compounds are known to have selective antiproliferative activity on tumor cell lines.[57–60] Thus, conjugates **2a-h** might be nontoxic or less toxic to primary (non-tumor) cell lines than to tumor ones as Huh-7 hepatocytes. A preliminary assessment of the cytotoxicity of these compounds to different tumor cell lines and one primary cell line, showed them to have a selective effect against cancer cells (undisclosed data). In other words, one cannot rule out the possibility that conjugates **2a-h** could have a selective action against hepatic forms of *Plasmodium* inside the liver cells.

2.2.3. Gametocytocidal activity

The gametocytocidal activity of compounds **2a-h** was assessed *in vitro* against early gametocytes of the *P. falciparum* NF54-*gexp02-Tom* strain, which contains a fluorescent protein that is under the control of a gametocyte-specific promoter leading to accurate and easy-to-perform quantification of gametocytes.[61] While a dose-dependent response was observed in all cases, reliable IC_{50} values could only be determined for compounds **2a**, **2d**, **2f,** and **2 g**. Remarkably, the IC_{50} values obtained for conjugates **2** (0.645 μM > IC_{50} > 0.461 μM) were at least 25-fold lower than that of the reference drug in this stage, PQ (IC_{50} = 17.66 ± 2.31 μM). Indeed, compounds that can efficiently eliminate gametocytes remain scarce, while they play a crucial role in preventing host-to-vector transmission.[62].

3. Concluding remarks

We disclose a new family of compounds (**2a-h**) as promising multi-stage antiplasmodial leads. These compounds were obtained by coupling different *trans*-cinnamic acids to 4,9-diaminoacridines previously identified as dual-stage antiplasmodial hits. Considering our earlier findings on the enhancement of the antiplasmodial activity of 4-aminoacridines through their coupling to cinnamic acids,[39] we hypothesized that using the same strategy on 4,9-aminoacridines **1a,b** could have a similar outcome. Overall, the data herein reported support the validity of this working hypothesis, since the conjugates **2a-h** exhibit enhanced multi-stage activity *in vitro*, especially against the erythrocytic and gametocyte stages, compared to the parent compounds **1a** and **1b**. While conjugate **2 h** (n = 2, R = H, R_1 = H) displayed the highest activity against blood stage parasites, conjugate **2 g** (n = 2, R = H, R_1 = *m*-F), which only differs from the former in the substituent R_1 of the aryl ring, showed the best combined activity against the blood and gametocyte stages of *P. falciparum*.

The activity against hepatic forms of *P. berghei* was also noteworthy, despite the high toxicity observed towards Huh-7 cells, which might not be observed in the case of primary (non-tumor) cell lines. This hypothesis is under investigation and preliminary undisclosed data support a selective action of conjugates **2a-h** against tumor cells.

The MOA(s) behind the multi-stage antiplasmodial activity of conjugates **2a-h** remain unknown. The significant differences in blood- and liver-stage activities between the conjugates herein reported (**2a-h**) and their earlier analogues derived from 4-aminoacridines (**3a-d**) highlight the influence of the aminoalkyl chain linked to the C-9 position of the acridine ring, but cannot be interpreted as indicative of similar or dissimilar MOA(s). The positive influence of this chain on blood stage activity could be related to an improved compound accumulation inside the acidic digestive vacuole of the parasite, followed by inhibition of hemozoin formation. However, other alternative or additional MOA(s) can be considered, such as the ability of cinnamic acids to (i) hinder the production of ATP, (ii) reduce the translocation of amino acids and carbohydrates to parasitized erythrocytes, (iii) upset the parasite's mitochondrial respiration, and (iv) inhibit cysteine proteases in intra-erythrocytic parasites.[40,43–48] Additionally, the planar acridine ring present in QN analogues like **2a-h**, is reported as capable of intercalating with DNA, which may account for the bioactivity of these conjugates.[57–60] Yet, these are new molecular entities that may owe their multi-stage antiplasmodial action to other mechanisms beyond those reported for structurally related compounds. Ongoing studies (undisclosed data) will hopefully shed some light into this matter.

In conclusion, the results herein reported highlight compounds **2a-h** as new multi-stage antiplasmodial hits. Given the importance of halting

the infection's progression within the human host from its very beginning in the liver and through its symptomatic stage in red blood cells to the gametocyte stage underlying disease propagation, these findings are a significant step forward towards the development of new valuable antiplasmodial candidates.

4. Experimental section

4.1. Chemistry

4.1.1. Synthesis of compounds 1a-b

4-(4-aminobutyl)amino-6-chloro-9-[*N*-(4-(diethylamino)pent-2-yl] amino-2-methoxy-acridine (**1a**) and 4-(4-aminobutyl)amino-6-chloro-9-[*N*-(3-(diethylamino)prop-1-yl]amino-2-methoxy-acridine (**1b**) were prepared by a seven-step route as previously described and optimized by us, and their structural analyses (see SI) agreed with formerly reported data.[38,49].

4.1.2. Synthesis of compounds 2a-h

The *trans*-cinnamic acid of interest (1 equiv) was dissolved in DCM and then TBTU (1.1 equiv) and DIEA (2 equiv) were added. Following an activation period of about 1 h, compound **1a** or **1b** (1 equiv) in DCM was added to the mixture and the reaction proceeded under stirring at r.t. until no additional advancement could be detected by thin-layer chromatography (TLC) (1–3 h). Next, the mixture underwent successive washes with saturated aq. $NaHCO_3$ (3 × 50 mL) and saturated aq. NaCl (3 × 50 mL), and the organic layers were pooled, dried over anhydrous Na_2SO_4, and filtered by gravity. The resulting filtrate was concentrated to dryness under reduced pressure. The crude product thus obtained was subjected to purification by column chromatography on silica gel using an elution mixture of DCM/CH_3OH 8:1 (v/v). This process yielded compounds **2a-h** with purity degrees ranging from 94 % to 99 % (HPLC) and correct structural data (NMR and ESI-IT-MS), as given in detail below. Chromatographic and spectral traces are provided in the SI.

4.1.2.1. Compound 2a. Orange oil, η = 42 % (0.0093 g); **^{1}H NMR** (400 MHz, $CDCl_3$) δ 8.11 (bs, 1H), 8.00 (d, J = 9.2 Hz, 1H), 7.55 (d, J = 15.6 Hz, 1H), 7.48 – 7.39 (m, 2H), 7.30 – 7.26 (m, 2H), 7.05 – 6.96 (m, 2H), 6.64 – 6.53 (m, 2H), 6.41 (d, J = 15.6 Hz, 1H), 6.25 (d, J = 2.2 Hz, 1H), 4.08 – 3.99 (m, 1H), 3.94 (s, 3H), 3.46 (q, J = 6.4 Hz, 2H), 3.34 – 3.23 (m, 2H), 2.92 (q, J = 7.9, J = 7.3 Hz, 4H), 2.87 – 2.80 (m, 2H), 1.94 – 1.73 (m, 9H), 1.32 (d, J = 6.3 Hz, 3H), 1.19 (t, J = 7.3 Hz, 6H); **^{13}C NMR** (101 MHz, $CDCl_3$) δ 166.22, 164.78, 162.30, 158.59, 139.46, 131.37, 129.65, 125.10, 124.77, 120.97, 116.04, 115.82, 55.74, 55.43, 52.04, 46.87, 43.43, 39.67, 35.44, 29.83, 27.57, 26.37, 22.82, 22.35, 21.25, 14.24, 8.67, 1.15; **$^m/_z$ (ESI-IT MS, +)** 634.87 (M + H^+); M^+ ($C_{36}H_{45}ClFN_5O_2$) requires 633.32; **HPLC-DAD:** RT, 15.550 min; purity degree (peak relative area), 97.9 %.

4.1.2.2. Compound 2b. Orange oil, η = 24 % (0.0066 g); **^{1}H NMR** (400 MHz, $CDCl_3$) δ 8.18 (bs, 1H), 8.02 (d, J = 9.2 Hz, 1H), 7.79 – 7.72 (m, 1H), 7.64 – 7.57 (m, 1H), 7.55 (d, J = 15.5 Hz, 1H), 7.45 – 7.37 (m, 2H), 7.25 – 7.22 (m, 1H), 6.87 – 6.81 (m, 2H), 6.70 (s, 1H), 6.56 (bs, 1H), 6.40 (d, J = 15.6 Hz, 1H), 6.27 (d, J = 2.2 Hz, 1H), 4.18 – 4.08 (m, 1H), 3.90 (s, 3H), 3.81 (s, 3H), 3.47 (q, J = 6.3 Hz, 2H), 3.28 (t, J = 6.4 Hz, 2H), 2.96 (q, J = 7.5, 6.6 Hz, 4H), 2.88 (t, J = 7.3 Hz, 2H), 2.05 – 1.60 (m, 8H), 1.37 (d, J = 6.3 Hz, 3H), 1.20 (t, J = 7.3 Hz, 6H); **^{13}C NMR** (101 MHz, $CDCl_3$) 166.87, 160.90, 158.54, 140.36, 129.49, 127.95, 127.84, 125.14, 125.05, 125.01, 118.86, 114.33, 55.78, 55.54, 55.48, 52.08, 46.83, 43.72, 39.64, 35.27, 27.68, 26.11, 22.27, 21.30, 8.54, 1.16; **$^m/_z$ (ESI-IT MS, +)** 646.67 (M + H^+); M^+ ($C_{37}H_{48}ClN_5O_3$) requires 645.34; **HPLC-DAD:** RT, 15.590 min; purity degree (peak relative area), 94.3 %.

4.1.2.3. Compound 2c. Orange oil, η = 44 % (0.0122 g); **^{1}H NMR** (400 MHz, $CDCl_3$) δ 8.09 (bs, 1H), 7.99 (d, J = 9.2 Hz, 1H), 7.54 (d, J = 15.7 Hz, 1H), 7.34 – 7.10 (m, 6H), 7.04 – 6.95 (m, 1H), 6.60 – 6.52 (m, 2H), 6.47 (d, J = 15.6 Hz, 1H), 6.24 (d, J = 2.2 Hz, 1H), 4.10 – 3.98 (m, 1H), 3.93 (s, 3H), 3.47 (q, J = 6.4 Hz, 2H), 3.35 – 3.25 (m, 2H), 2.93 (q, J = 7.5 Hz, 4H), 2.84 (t, J = 7.5 Hz, 2H), 1.95 – 1.57 (m, 8H), 1.32 (d, J = 6.4 Hz, 3H), 1.20 (t, J = 7.3 Hz, 6H); **^{13}C NMR** (101 MHz, $CDCl_3$) δ 165.93, 164.32, 161.88, 158.58, 139.40, 139.37, 137.51, 137.43, 130.46, 130.38, 125.13, 124.72, 124.07, 124.05, 122.61, 116.53, 116.32, 114.11, 113.89, 55.69, 55.39, 52.08, 46.89, 43.38, 39.72, 35.49, 29.83, 27.51, 26.39, 22.35, 21.26, 8.67, 1.15; **$^m/_z$ (ESI-IT MS, +)** 634.40 (M + H^+); M^+ ($C_{36}H_{45}ClN_5O_2$) requires 633.32; **HPLC-DAD:** RT, 15.610 min; purity degree (peak relative area), 97.0 %.

4.1.2.4. Compound 2d. Orange oil, η = 39 % (0.0079 g); **^{1}H NMR** (400 MHz, $CDCl_3$) δ 8.07 (bs, 1H), 7.99 (d, J = 9.2 Hz, 1H), 7.59 (d, J = 15.6 Hz, 1H), 7.50 – 7.43 (m, 2H), 7.35 – 7.27 (m, 5H), 6.59 – 6.50 (m, 2H), 6.47 (d, J = 15.6 Hz, 1H), 6.36 (bs, 1H), 6.24 (d, J = 2.3 Hz, 1H), 4.07 – 3.98 (m, 1H), 3.93 (s, 3H), 3.46 (q, J = 6.5 Hz, 2H), 3.34 – 3.24 (m, 2H), 2.91 (q, J = 7.3 Hz, 4H), 2.83 (t, J = 7.5 Hz, 2H), 1.91 – 1.57 (m, 8H), 1.30 (d, J = 6.4 Hz, 3H), 1.18 (t, J = 7.3 Hz, 6H); **^{13}C NMR** (101 MHz, $CDCl_3$) δ 166.35, 158.59, 144.95, 140.82, 135.07, 129.67, 128.90, 127.93, 125.11, 124.73, 121.13, 86.63, 55.69, 55.40, 52.06, 46.88, 43.39, 39.67, 35.44, 29.83, 27.66, 26.37, 22.82, 22.32, 21.26, 14.24, 8.70; **$^m/_z$ (ESI-IT MS, +)** 616.41 (M + H^+); M^+ ($C_{36}H_{46}ClN_5O_2$) requires 615.33; **HPLC-DAD:** RT, 15.467 min; purity degree (peak relative area), 98.7 %.

4.1.2.5. Compound 2e. Orange oil, η = 43 % (0.0087 g); **^{1}H NMR** (400 MHz, $CDCl_3$) δ 8.25 (bs, 1H), 8.00 (d, J = 9.3 Hz, 1H), 7.56 (d, J = 15.7 Hz, 1H), 7.51 – 7.44 (m, 2H), 7.15 (dd, J = 9.3, 2.1 Hz, 1H), 7.04 – 6.97 (m, 3H), 6.70 (Bs, 1H), 6.64 (d, J = 2.3 Hz, 1H), 6.58 (d, J = 15.7 Hz, 1H), 6.28 (d, J = 2.1 Hz, 1H), 4.06 – 3.98 (m, 2H), 3.91 (s, 3H), 3.49 (q, J = 6.0 Hz, 2H), 3.31 – 3.21 (m, 2H), 2.95 – 2.86 (m, 6H), 2.14 – 1.80 (m, 6H), 1.20 (t, J = 7.2 Hz, 6H); **^{13}C NMR** (101 MHz, $CDCl_3$) δ 166.53, 164.72, 162.24, 158.04, 139.06, 131.54, 129.70, 125.60, 124.15, 121.37, 115.97, 115.76, 109.39, 55.85, 51.05, 47.08, 43.98, 39.73, 29.84, 27.37, 26.07, 25.65, 14.25, 9.79, 1.15; **$^m/_z$ (ESI-IT MS, +)** 606.93 (M + H^+); M^+ ($C_{34}H_{41}ClFN_5O_2$) requires 605.29; **HPLC-DAD:** RT, 14.910 min; purity degree (peak relative area), 94.4 %.

4.1.2.6. Compound 2f. Orange oil, η = 66 % (0.0105 g); **^{1}H NMR** (400 MHz, $CDCl_3$) δ 8.20 (bs, 1H), 8.00 (d, J = 9.3 Hz, 1H), 7.55 (d, J = 15.6 Hz, 1H), 7.47 – 7.41 (m, 2H), 7.13 (dd, J = 9.3, 2.1 Hz, 1H), 6.87 – 6.81 (m, 2H), 6.75 – 6.66 (m, 2H), 6.48 (d, J = 15.6 Hz, 1H), 6.25 (d, J = 2.2 Hz, 1H), 4.01 (t, J = 5.8 Hz, 2H), 3.90 (s, 3H), 3.80 (s, 3H), 3.48 (q, J = 6.1 Hz, 2H), 3.30 – 3.18 (m, 2H), 2.99 – 2.90 (m, 6H), 2.20 – 1.76 (m, 6H), 1.21 (t, J = 7.2 Hz, 6H); **^{13}C NMR** (101 MHz, $CDCl_3$) δ 166.96, 160.82, 158.13, 140.07, 129.50, 127.98, 124.22, 119.13, 114.30, 55.89, 55.46, 46.90, 43.95, 39.67, 29.84, 27.53, 26.05, 25.59, 9.45; **$^m/_z$ (ESI-IT MS, +)** 618.60 (M + H^+); M^+ ($C_{35}H_{44}ClN_5O_3$) requires 617.31; **HPLC-DAD:** RT, 14.950 min; purity degree (peak relative area), 97.6 %.

4.1.2.7. Compound 2 g. Orange oil, η = 82 % (0.0132 g); **^{1}H NMR** (400 MHz, $CDCl_3$) δ 8.25 (bs, 1H), 7.99 (d, J = 9.3 Hz, 1H), 7.55 (d, J = 15.7 Hz, 1H), 7.34 – 7.07 (m, 4H), 7.07 – 6.93 (m, 1H), 6.79 – 6.58 (m, 3H), 6.28 (d, J = 2.2 Hz, 1H), 4.02 (t, J = 5.6 Hz, 2H), 3.90 (s, 3H), 3.49 (q, J = 6.0 Hz, 2H), 3.34 – 3.18 (m, 2H), 3.00 – 2.86 (m, 6H), 2.17 – 1.80 (m, 6H), 1.20 (t, J = 7.2 Hz, 6H); **^{13}C NMR** (101 MHz, $CDCl_3$) δ 166.21, 164.33, 161.89, 158.08, 139.00, 137.66, 130.38, 130.30, 125.58, 124.21, 123.99, 123.02, 116.35, 116.13, 114.28, 114.07, 55.84, 47.00, 43.96, 39.76, 29.85, 27.27, 26.08, 25.62, 9.64; **$^m/_z$ (ESI-IT MS, +)** 606.47 (M + H^+); M^+ ($C_{34}H_{41}ClFN_5O_2$) requires 605.29; **HPLC-DAD:** RT, 15.040 min; purity degree (peak relative area), 97.0 %.

4.1.2.8. Compound 2 h. Orange oil, η = 33 % (0.0063 g); **^{1}H NMR** (400

MHz, $CDCl_3$) δ 8.26 (bs, 1H), 8.00 (d, $J = 9.3$ Hz, 1H), 7.61 (d, $J = 15.7$ Hz, 1H), 7.54 – 7.45 (m, 2H), 7.37 – 7.27 (m, 3H), 7.15 (dd, $J = 9.3$, 2.1 Hz, 1H), 6.81 – 6.55 (m, 3H), 6.27 (d, $J = 2.2$ Hz, 1H), 4.05 – 3.99 (m, 2H), 3.92 (s, 3H), 3.50 (q, $J = 6.1$ Hz, 2H), 3.29 – 3.24 (m, 2H), 2.94 – 2.85 (m, 6H), 2.15 – 1.81 (m, 6H), 1.20 (t, $J = 7.2$ Hz, 6H); **^{13}C NMR** (101 MHz, $CDCl_3$) δ 166.62, 158.05, 140.41, 135.29, 129.50, 128.85, 127.99, 125.54, 124.14, 121.53, 55.89, 47.01, 43.93, 39.74, 29.84, 27.40, 26.09, 25.66, 9.73, 1.15; **$^{m}/_{z}$ (ESI-IT MS)** 588.45 ($M + H^+$); M^+ ($C_{34}H_{42}ClN_5O_2$) requires 587.30; **HPLC-DAD:** RT, 14.760 min; purity degree (peak relative area), 94.4 %.

4.2. In vitro assays

4.2.1. Blood stage activity

Asexual stages of the *P. falciparum* 3D7 strain were grown in group B human erythrocytes at 3 % hematocrit using Roswell Park Memorial Institute 1640 medium (RPMI) supplemented with 0.5 % (w/v) Albumax II (Life Technologies, New Zealand) and 2 mM L-glutamine. During the full experiment, parasites were maintained in standard culturing conditions (37 °C, 5 % O_2, 5 % CO_2, and 90 % N_2). The parasites were first synchronized in the ring stage with a 5 % sorbitol lysis as described in ref.[63] Then, the newly established parasite culture (0.75 % parasitemia) was transferred to 96-well plates and incubated with growing concentrations of the different compounds (0.0051–100 μM). As control, parasites were left untreated. After 48 h of incubation, cultures were diluted to ca. 1–10 × 10^6 cells/mL and incubated with Syto11 to stain the nuclei. Parasitemia was measured by flow cytometry using a LSRFortessa flow cytometer (BD Biosciences, USA) equipped with the 4 lasers, 20 parameters standard configuration. The single-cell population was selected on a forward-side scattergram. Syto 11 fluorescence signal was detected by exciting samples at 488 nm and collecting the emission with a 530/30-nm bandpass filter. Growth inhibition was calculated by referencing the growth rates of a chloroquine-treated culture (100 % inhibition) and of an untreated culture (0 % inhibition). The obtained data were subjected to sigmoidal fitting using the GraphPad Prism 8.4.2 software, allowing the determination of the compounds concentrations required to reduce *P. falciparum* viability by 50 % (IC_{50}).

4.2.2. Hepatic stage activity

The *in vitro* inhibition of hepatic infection was assessed by measuring the luminescence intensity in lysates of Huh-7 cells infected with a firefly luciferase-expressing *P. berghei* line, *PbGFP*-Luccon, as previously described.[55,56] Briefly, Huh-7 cells were cultured in RPMI supplemented with 10 % v/v fetal calf serum, 1 % v/v penicillin/streptomycin, 1 % v/v nonessential amino acids, 1 % v/v glutamine, and 10 mM 4-(2-hydroxyethyl)-1-piperazine ethanesulfonic acid (HEPES), pH 7, and maintained at 37 °C with 5 % CO_2. Huh-7 cells were seeded in 96-well plates on the day before drug treatment and infection. About 1 h prior to infection with sporozoites freshly obtained by disruption of salivary glands of infected female *Anopheles stephensi* mosquitoes, the culture medium in the wells was replaced by infection medium (culture medium supplemented with 50 μg/mL gentamicin and 0.8 μg/mL amphotericin B) containing the suitable concentration of each compound. In control wells, the cell culture medium was replaced by a medium containing the same percentage of dimethyl sulfoxide (DMSO) used in compound solutions (0.01 %), which is not cytotoxic. Following a 48-h infection period, the compounds' effect on the viability of Huh-7 cells was assessed by the AlamarBlue assay (Invitrogen, UK) using the manufacturer's protocol, and infection was measured by a bioluminescence assay (Biotium, USA), also according to the manufacturer's instructions. Nonlinear regression analysis was employed to fit the normalized results of the dose–response curves, and IC_{50} values were determined using GraphPad Prism 8.4.2. software. From the extrapolation of cell confluency data, the cytotoxicity of tested compounds was assessed.

4.2.3. Gametocytocidal activity

P. falciparum parasites of the high-gametocyte productive NF54-gexp02-Tom line (kindly supplied by Prof. Alfred Cortés) were utilized. This line features a genome-integrated tandem Tomato (tdTomato) fluorescent marker gene controlled by an early gametocyte promoter (gexp02).[61] The parasites were cultured in group B human erythrocytes at 3 % hematocrit using RPMI-based standard medium supplemented with 2 mM choline chloride, and incubated at 37 °C under hypoxic conditions (5 % O_2, 5 % CO_2, and 90 % N_2 at 37 ∘C). To induce sexual conversion, choline was removed from the medium, accompanied by synchronization through sorbitol lysis, and addition of 10 % Human serum. Subsequently, the induced cultures were then maintained without choline until the end of the experiment. The impact on gametocyte development was evaluated in three independent replicas by adding growing concentrations (0.0051–100 μM) of each compound to the culture. The appearance of stage V gametocytes was daily monitored by light microscopy, and approximately fifteen days after choline removal, nearly 80 % of gametocytes reached stages IV and V (mature forms). After this time, Giemsa-stained blood smears were prepared and at least 10,000 cells were manually counted for each condition. A positive control treated with the IC_{90} of PQ and a negative control culture without drugs were also included in the experiment. Growth inhibition was calculated as the total parasitemia relative to control cultures and expressed as a percentage. The data were then subjected to sigmoidal fitting to determine the IC_{50} values of compounds **2a-h**, using the GraphPad Prism 8.4.2. software.

Funding

This work received financial support from PT national funds (FCT/MCTES, Fundação para a Ciência e Tecnologia and Ministério da Ciência, Tecnologia e Ensino Superior) through project CIRCNA/BRB/0281/2019.

CRediT authorship contribution statement

Mélanie Fonte: Writing – original draft, Validation, Methodology, Investigation, Formal analysis, Data curation. **Catarina Rôla:** Methodology, Investigation, Data curation. **Sofia Santana:** Writing – original draft, Validation, Methodology, Investigation, Data curation. **Yunuen Avalos-Padilla:** Validation, Methodology, Investigation, Formal analysis, Data curation, Writing – original draft. **Xavier Fernàndez-Busquets:** Conceptualization, Formal analysis, Funding acquisition, Supervision, Validation, Writing – review & editing. **Miguel Prudêncio:** Writing – review & editing, Validation, Supervision, Funding acquisition, Formal analysis. **Paula Gomes:** . **Cátia Teixeira:** Writing – review & editing, Validation, Supervision, Investigation, Formal analysis, Conceptualization.

Declaration of competing interest

The authors declare that they have no known competing financial interests or personal relationships that could have appeared to influence the work reported in this paper.

Data availability

Data will be made available on request.

Acknowledgments

The authors thank FCT/MCTES for supporting Research Units LAQV-REQUIMTE (LA/P/0008/2020 DOI 10.54499/LA/P/0008/2020, UIDP/50006/2020 DOI 10.54499/UIDP/50006/2020 and UIDB/50006/2020 DOI 10.54499/UIDB/50006/2020) and for the Doctoral Grant to MF (SRFH/BD/147354/2019). MP further acknowledges the "la Caixa"

Foundation for Grant HR21-848. ISGlobal and IBEC are members of the CERCA Programme, Generalitat de Catalunya. We acknowledge support from the Ministerio de Ciencia e Innovación/Agencia Estatal de Investigación (MCIN/AEI/ 10.13039/501100011033) through the "Centro de Excelencia Severo Ochoa 2019-2023" Program (CEX2018-000806-S). This research is part of ISGlobal's Program on the Molecular Mechanisms of Malaria which is partially supported by the Fundación Ramón Areces.

Appendix A. Supplementary data

Supplementary data to this article can be found online at https://doi.org/10.1016/j.bmc.2024.117714.

References

1. World Health Organization, World malaria report, 2023.
2. Dhiman S. *Infect Dis Poverty*. 2019;8:14.
3. Antony HA, Parija SC. *Tropical Parasitology*. 2016;6:30–41.
4. World Health Organization, Artemisinin resistance and artemisinin-based combination therapy efficacy, 2018.
5. Balikagala B, Fukuda N, Ikeda M, et al. *N Engl J Med*. 2021;385:1163–1171.
6. Noreen N, Ullah A, Salman SM, Mabkhot Y, Alsayari A, Badshah SL. *Journal of Global Antimicrobial Resistance*. 2021;27:142–149.
7. Nsanzabana C. *Trop Med Infect Dis*. 2019;4:26.
8. Rosenthal PJ. *Lancet Infect Dis*. 2021;21:1056–1057.
9. Rosenthal PJ. *Am J Trop Med Hyg*. 2022;106:1565–1567.
10. King K. Holmes, S. Bertozzi, Barry R. Bloom, et al. Major Infectious Diseases: Key Messages from Disease Control Priorities. In: King K. Holmes, S. Bertozzi, Barry R. Bloom, Prabhat Jha, eds. 3 ed.; ch. 12 - *Malaria Elimination and Eradication*, 2017.
11. Burrows JN, Duparc S, Gutteridge WE, et al. *Malar J*. 2017;16:26.
12. Tibon NS, Ng CH, Cheong SL. *Eur J Med Chem*. 2020;188, 111983.
13. Makhoba XH, Viegas Jr C, Mosa RA, Viegas FPD, Pooe OJ. Drug design. *Development and Therapy*. 2020;14:3235–3249.
14. Talevi A. *Front Pharmacol*. 2015:6.
15. Siqueira-Neto JL, Wicht KJ, Chibale K, Burrows JN, Fidock DA, Winzeler EA. *Nat Rev Drug Discov*. 2023;22:807–826.
16. Teixeira C, Vale N, Pérez B, Gomes A, Gomes JRB, Gomes P. *Chem Rev*. 2014;114:11164–11220.
17. Pinheiro L, Feitosa L, Gandi M, Silveira F, Boechat N. *Molecules*. 2019:24.
18. Pandey SK, Anand U, Siddiqui WA, Tripathi R. *Advances in Medicine*. 2023;2023, 5060665.
19. Araújo MJ, Bom J, Capela R, et al. *J Med Chem*. 2005;48:888–892.
20. Matos J, Cruz FPD, Cabrita É, Gut J, Nogueira F, Rosário VED, Moreira R, Rosenthal PJ, Prudêncio M, Gomes P. *Antimicrob Agents Chemother*. 2012;56:1564–1570.
21. Vale N, Nogueira F, do Rosário VE, Gomes P, Moreira R. *Eur J Med Chem*. 2009;44:2506–2516.
22. Vale N, Prudêncio M, Marques CA, et al. *J Med Chem*. 2009;52:7800–7807.
23. Fonte M, Tassi N, Fontinha D, et al. *ChemMedChem*. 2021;16:788–792.
24. Gomes A, Machado M, Lobo L, et al. *ChemMedChem*. 2015;10:1344–1349.
25. Gomes A, Pérez B, Albuquerque I, et al. *ChemMedChem*. 2014;9:305–310.
26. Pérez B, Teixeira C, Albuquerque IS, et al. *MedChemComm*. 2012;3:1170–1172.
27. Pérez B, Teixeira C, Gomes AS, et al. *Bioorg Med Chem Lett*. 2013;23:610–613.
28. Pérez B, Teixeira C, Gut J, Rosenthal PJ, Gomes JRB, Gomes P. *ChemMedChem*. 2012;7:1537–1540.
29. Pérez B, Teixeira C, Albuquerque IS, et al. *J Med Chem*. 2013;56:556–567.
30. Pérez B, Teixeira C, Figueiras M, et al. *Eur J Med Chem*. 2012;54:887–899.
31. Fonte M, Tassi N, Gomes P, Teixeira C. *Molecules*. 2021;26:600.
32. Parvathaneni V, Kulkarni NS, Muth A, Gupta V. *Drug Discov Today*. 2019;24:2076–2085.
33. D. A. van Schalkwyk, in *Encyclopedia of Life Sciences*, pp. 1-5.
34. Schlitzer M. *ChemMedChem*. 2007;2:944–986.
35. Mayence A, Vanden eynde JJ. *Pharmaceuticals*. 2019;12:115.
36. Ashley EA, Recht J, White NJ. *Malar J*. 2014;13:418.
37. Vale N, Moreira R, Gomes P. *Eur J Med Chem*. 2009;44:937–953.
38. Fonte M, Fagundes N, Gomes A, et al. *Tetrahedron Lett*. 2019;60:1166–1169.
39. Fonte M, Fontinha D, Moita D, et al. *Eur J Med Chem*. 2023;258, 115575.
40. Ruwizhi N, Aderibigbe BA. *Int J Mol Sci*. 2020;21:5712.
41. Meunier B. *Polypharmacology in Drug Discovery*. 2012:423–439.
42. Meunier B. *Acc Chem Res*. 2008;41:69–77.
43. Kanaani J, Ginsburg H. *Antimicrob Agents Chemother*. 1992;36:1102–1108.
44. Silva AT, Bento CM, Pena AC, et al. *Molecules*. 2020;25:66.
45. De P, Bedos-Belval F, Vanucci-Bacque C, Baltas M. *Curr Org Chem*. 2012;16:747–768.
46. Santos MM, Moreira R. *Mini-Rev Med Chem*. 2007;7:1040–1050.
47. Rosenthal PJ, Olson JE, Lee GK, Palmer JT, Klaus JL, Rasnick D. *Antimicrob Agents Chemother*. 1996;40:1600–1603.
48. Previti S, Ettari R, Cosconati S, et al. *J Med Chem*. 2017;60:6911–6923.
49. Fonte M, Teixeira C, Gomes P. *RSC Adv*. 2024;14:6253–6261.
50. Coronado LM, Nadovich CT, Spadafora C. Biochimica et biophysica acta (BBA). - *General Subjects*. 1840, 2014,:2032–2041.
51. Deshpande S, Kay B. *Med Chem*. 2016:6.
52. Hu Y-Q, Gao C, Zhang S, et al. *Eur J Med Chem*. 2017;139:22–47.
53. Agnello S, Brand M, Chellat M, Gazzola S, Riedl R. *Angew Chem Int Ed*. 2018:58.
54. Rawe SL, McDonnell C. In: *G*. L. Patrick: Elsevier; 2020:65–98.
55. Ploemen IHJ, Prudêncio M, Douradinha BG, et al. *PLoS One*. 2009;4:e7881.
56. Prudêncio M, Mota MM, Mendes AM. *Trends Parasitol*. 2011;27:565–574.
57. Ehsanian R, Van Waes C, Feller SM. *Cell Communication and Signaling*. 2011;9:13.
58. Gomes A, Fernandes I, Teixeira C, Mateus N, Sottomayor MJ, Gomes P. *ChemMedChem*. 2016;11:2703–2712.
59. Kumar M, Sarkar A. *Sci Pharm*. 2022;90:12.
60. Kumar R, Kaur M, Kumari M. *Acta Pol Pharm*. 2012;69:3–9.
61. Portugaliza HP, Llorà-Batlle O, Rosanas-Urgell A, Cortés A. *Sci Rep*. 2019;9:14595.
62. Munro BA, McMorran BJ. *Parasitologia*. 2022;2:101–124.
63. Lambros C, Vanderberg JP. *J Parasitol*. 1979;65:418–420.